## General Disclaimer

## One or more of the Following Statements may affect this Document

- This document has been reproduced from the best copy furnished by the organizational source. It is being released in the interest of making available as much information as possible.

- This document may contain data, which exceeds the sheet parameters. It was furnished in this condition by the organizational source and is the best copy available.

- This document may contain tone-on-tone or color graphs, charts and/or pictures, which have been reproduced in black and white.

- This document is paginated as submitted by the original source.

- Portions of this document are not fully legible due to the historical nature of some of the material. However, it is the best reproduction available from the original submission.

NASA CR-135277
PWA-5540

# EXPERIMENTAL CLEAN COMBUSTOR PROGRAM
# TURBULENCE CHARACTERISTICS OF COMPRESSOR DISCHARGE FLOWS

by

P. S. Follansbee and R. R. Dils

UNITED TECHNOLOGIES CORPORATION
Pratt & Whitney Aircraft Group
Commercial Products Division



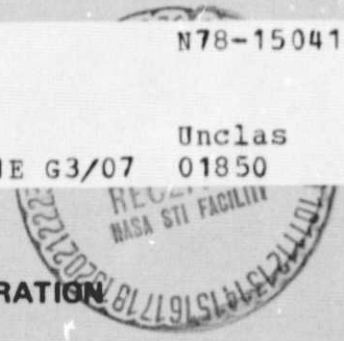

Prepared for
NATIONAL AERONAUTICS AND SPACE ADMINISTRATION
NASA-Lewis Research Center
Contract NAS3-19447

**PRATT & WHITNEY AIRCRAFT GROUP**

East Hartford, Connecticut 06108

25 January 1978

To: National Aeronautics and Space Administration
Lewis Research Center
21000 Brookpark Road
Cleveland, Ohio 44135

Attention: Mr. Francis O. Driscoll, Mail Stop 500-206

Subject: Final Report on Turbulence Characteristics of Compressor Discharge Flows (NASA CR-135277, PWA-5540) for the Experimental Clean Combustor Program, Phase III

Reference: Contract NAS3-19447, Modification 1

Attachment: One (1) Copy of the subject final report

Gentlemen:

Exclosed herewith is one (1) copy of the subject report and one (1) set of glossy continuous tone prints of all photographs included in the subject report. This report and the set of glossy continuous tone prints are submitted to fulfill the requirements of the Reports of Work Section Paragraph C (5) of the referenced contract.

Distribution of this report is being made in accordance with the distribution list furnished by the National Aeronautics and Space Administration Contracting Office. The distribution list is included at the end of the report.

Sincerely yours,

UNITED TECHNOLOGIES CORPORATION
Pratt & Whitney Aircraft Group
Commercial Products Division

A. Fiorentino

A. J. Fiorentino
Program Manager

cc: NASA-Lewis Research Center (Letter Only)
Cleveland, Ohio 44135
Attn: Mr. R. W. Niedzwiecki (MS 60-6)

Administrative Contracting Officer (Letter Only)
Air Force Plant Representative Office
Pratt & Whitney Aircraft Group
East Hartford, Connecticut 06108

UNITED TECHNOLOGIES

| 1. Report No. | 2. Government Accession No. | 3. Recipient's Catalog No. |
|---|---|---|
| NASA CR-135277 | | |

| 4. Title and Subtitle | 5. Report Date |
|---|---|
| EXPERIMENTAL CLEAN COMBUSTOR PROGRAM – TURBULENCE CHARACTERISTICS OF COMPRESSOR DISCHARGE FLOWS | October 1977 |
| | 6. Performing Organization Code |

| 7. Author(s) | 8. Performing Organization Report No. |
|---|---|
| P. S. Follansbee and R. R. Dils | PWA-5540 |
| | 10. Work Unit No. |

| 9. Performing Organization Name and Address | 11. Contract or Grant No. |
|---|---|
| UNITED TECHNOLOGIES CORPORATION<br>Pratt & Whitney Aircraft Group<br>Commercial Products Division<br>East Hartford, Connecticut 06108 | NAS3-19447 |
| | 13. Type of Report and Period Covered |
| 12. Sponsoring Agency Name and Address | Contractor Report |
| NATIONAL AERONAUTICS AND SPACE ADMINISTRATION<br>Lewis Research Center<br>21000 Brookpark Road, Cleveland, Ohio 44135 | 14. Sponsoring Agency Code |

15. Supplementary Notes

Project Manager, L. A. Diehl, NASA-Lewis Research Center, Cleveland, Ohio

16. Abstract

The results of turbulence measurements at the entrance to the diffuser duct of a large gas turbine are presented in this report. Hot film and hot wire measurements were conducted over a compressor discharge temperature range of 450K (idle) to 608K (rich approach). It was found that the turbulent intensity at the I.D. (25 percent span) and mid span locations increases gradually from 6 ±1 percent at idle to 7 ±1 percent at approach; the turbulent intensity at the O.D. (75 percent span) location increases from 7.5 ±0.5 percent at idle to 15 ±0.5 percent at approach. The energy in the velocity waves is uniformly distributed over a 0.1 to 5 kHz bandwidth and the cut-off frequency is not a strong function of the engine operation. The axial length of the fourier components within this bandwidth varies from 0.021 to 1.05m. The turbulence near the diffuser O.D. is of sufficient amplititude and scale to affect the flow to the front end sections of the burner.

| 17. Key Words (Suggested by Author(s)) | 18. Distribution Statement |
|---|---|
| Turbulent intensity<br>Turbulence<br>Cut-off frequency | Unclassified – Unlimited |

| 19. Security Classif. (of this report) | 20. Security Classif. (of this page) | 21. No. of Pages | 22. Price* |
|---|---|---|---|
| Unclassified | Unclassified | 48 | |

* For sale by the National Technical Information Service, Springfield, Virginia 22151

## FOREWORD

This document describes the work performed by the Commercial Products Division, Pratt & Whitney Aircraft Group of United Technologies Corporation under the Turbulence Measurement Addendum to Phase III of the Experimental Clean Combustor Program. This final report was prepared in accordance with Modification No. 1 to National Aeronautics and Space Administration, Lewis Research Center Contract NAS3-19447. This report has been assigned Commercial Products Division, Pratt & Whitney Aircraft Group internal report number PWA-5540.

Appreciation is expressed for the contributions made by Mr. Howard P. Grant of the Dynamic Measurements Development and Support Group at Pratt & Whitney Aircraft.

## TABLE OF CONTENTS

## LIST OF ILLUSTRATIONS

## LIST OF ILLUSTRATIONS (Cont'd)

## LIST OF TABLES

## SUMMARY

The results of turbulence measurements at the entrance to the diffuser duct of a JT9D gas turbine engine are presented in this report. A series of hot film and hot wire measurements were made with state-of-the-art probes over the range of engine operating conditions permitted by the probe endurance. The measurements were made in the experimental JT9D-20 engine X686 used for the Phase III Experimental Clean Combustor Program. Three engine tests were conducted from Idle ($T_4$ = 450K) to rich approach (608K). Several features of the turbulence in the diffuser duct were documented:

1. The turbulent intensity at the I.D. (25 percent span) and midspan locations increases gradually from 6 ±1 percent at idle to 7 ±1 percent at approach; the turbulent intensity at the O.D. (75 percent span) location increases from 7.5 ±0.5 percent at idle to 15 ±0.5 percent at approach.

2. The energy in the velocity waves is uniformly distributed over a 0.1 to 5 kHz bandwidth. The axial length of the fourier component within this bandwidth varies from 0.021 to 1.05 m.

3. The cut-off frequency of the turbulence (-3 db) is approximately 3 kHz and is not a function of the engine operation. Above the cut-off frequency, the fourier components of the wave decrease at a rate proportional to $f^{-2.5\pm0.1}$. Ninety percent of the energy of the waves is contained within a 0.1 to 5 kHz bandwidth.

4. Determination of the origin of the high level of turbulence at the diffuser O.D. requires further information on the development of the turbulence along the diffuser.

5. The turbulence at the diffuser O.D. is of sufficient amplitude and scale to affect the flow to the front end sections of the burner.

## INTRODUCTION

The objective of this addendum to the Phase III Experimental Clean Combustor Program was to conduct a series of measurements in order to document the turbulence characteristics of the compressor discharge flows within a JT9D engine. This report describes the program conducted and the results. The turbulent intensity and scale are of interest to advanced lean burning prevaporized-premixed combustor designs because of their potential effect on the fuel prevaporization and premixing near the entrance of a combustor and attendant changes in emissions performance.

This report is organized in four chapters. A summary of the program plan and schedule is presented in Chapter I. Chapter II contains a description of the experimental JT9D engine and turbulence measurement probes used for the program work and a description of the test and analysis procedures. The turbulence program results are discussed in Chapter III and the concluding remarks are presented in Chapter IV.

# CHAPTER I

# PROGRAM DESCRIPTION

## A. PHASE III ECCP PROGRAM

The turbulence program addendum was conducted concurrently with the latter stages of the Experimental Clean Combustor Program (ECCP) Phase III, which is described in a separate report [Reference 1].

The ECCP Phase III program, consisted of a detailed evaluation of a low pollution combustor, fuel system, and fuel control concept in a JT9D engine. The general objective was to demonstrate significant pollution reductions with an advanced combustor which meets the performance, operation, and installation requirements of the engine. The test program included steady-state and transient pollution and performance evaluations. Details of the work are contained in Reference 1. The turbulence measurements were made during the acceleration/deceleration test portion of the ECCP program.

## B. TURBULENCE MEASUREMENT PROGRAM

The turbulence measurement program was conducted during the second half of 1976. A series of hot film and hot wire measurements were made with state-of-the-art probes over the range of engine operating conditions permitted by the endurance of the sensing probes.

The program was accomplished in four tasks: Task I, Instrumentation, included the procurement, fabrication, and calibration of the required hot wire/hot film type probes; Task II, Testing and Data Acquisition, with the engine operating in a steady-state mode and at power levels ranging from sub-idle to the maximum consistent with the probe design; Task III, Data Analysis; and Task IV, Reporting.

## CHAPTER II

## EQUIPMENT AND EXPERIMENTAL PROCEDURES

### A. TEST ENGINE AND COMBUSTOR

Experimental JT9D-20 engine X-686 was used as the test vehicle for the Phase III Experimental Clean Combustor Program and the turbulence measurement addendum program. A detailed description of the engine is available in reference 1; a cross sectional schematic of a JT9D-7A reference engine is shown in Figure 1.

A flight-type nacelle normally was not employed for either experimental or production JT9D engine testing. A cylindrical core engine exhaust nozzle was used in place of the plug-type flight design; a pair of bifurcated fan ducts was used in place of the annular fan duct. The fan and core nozzle areas were sized to provide aerodynamic characteristics equivalent to the flight nacelles. The bifurcated fan ducts facilitate installation of special instrumentation and test hardware, and are readily removed for access to the core engine. The instrumented engine shown with the bifurcated fan ducts installed and ready for test is shown in Figure 2.

The engine was run in the P-6 test stand in an ambient inlet indoor test cell located at the Pratt & Whitney Aircraft facility in Middletown, Connecticut. The cell contains the instrumentation and data processing equipment required for the automatic temperature recording system and low-emission combustor development programs. The facility is equipped with a monorail engine handling system to facilitate movement of the engine into and out of the test cell. A schematic view of the test cell layout is shown in Figure 3. All engine controls, data logging, and computer face equipment are located in the test cell control room.

Cross section drawings of the Phase III Vorbix (vortex burning and mixing) combustor is shown in Figure 4. The Vorbix concept incorporates two burning zones separated axially by a high velocity throat section. The pilot zone is a conventional swirl-stabilized, direct-injection combustor employing thirty fuel injectors. It is sized to provide the required heat release rate for idle operation at high efficiency. Emissions of carbon monoxide and unburned hydrocarbons are minimized at idle operation conditions primarily by maintaining a sufficiently high pilot zone equivalence ratio to allow complete burning of the fuel.

At high power conditions, the pilot exhaust equivalence ratio was reduced as low as 0.3 (including pilot dilution air) to minimize formation of oxides of nitrogen. The minimum equivalence ratio for the pilot zone was determined by the overall lean blowout limits, combustion efficiency, and the need to maintain sufficient pilot zone temperature to vaporize and ignite the main zone fuel. Main zone fuel was introduced through fuel injectors located at the outer wall of the liner downstream of the pilot zone discharge location. Sixty fuel injectors were used. Main zone combustion and dilution air was introduced through sixty swirlers positioned on each side of the combustor. A more extensive description of the equipment, hardware and test procedures is found in the companion ECCP Final Report [Reference 1].

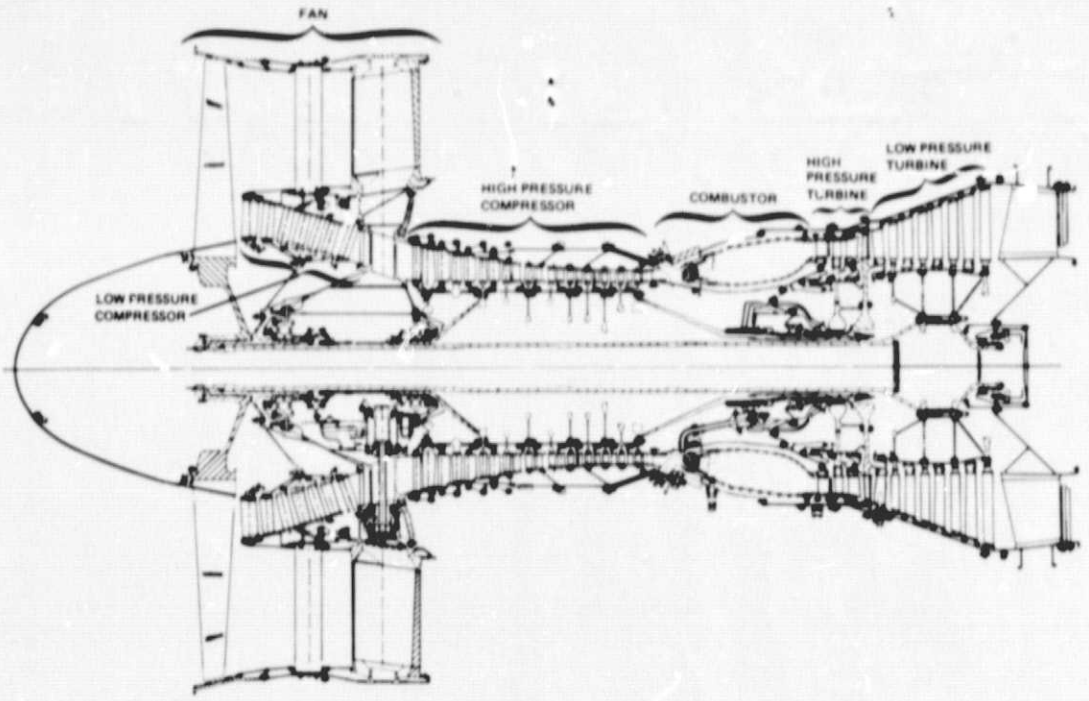


*Figure 1* *Cross Sectional Schematic of the JT9D-7A Reference Engine*

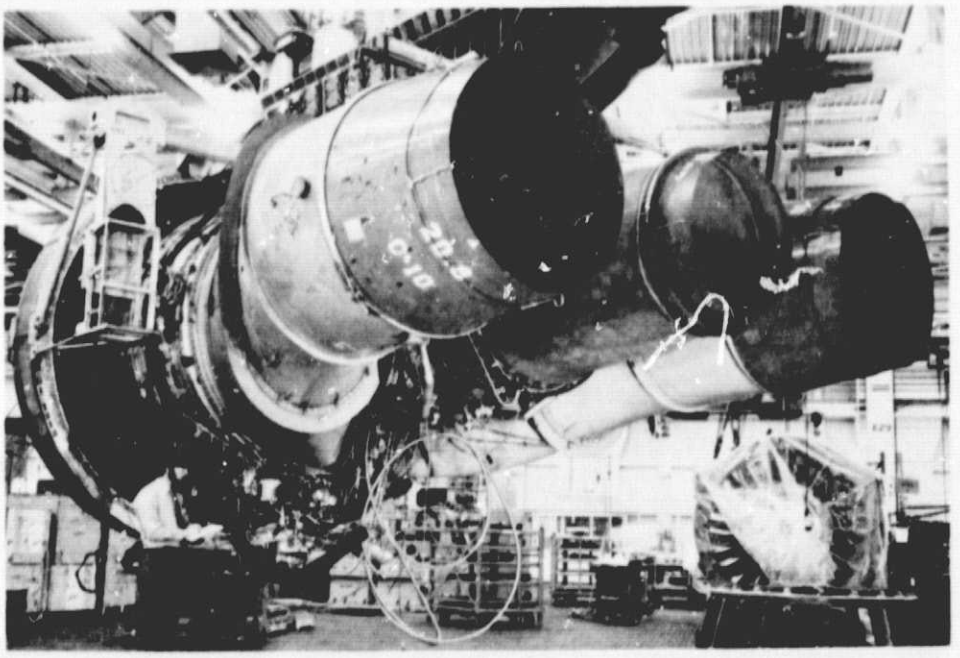

*Figure 2* *Experimental Engine, X-686, With Bifurcated Ducts Installed* *(X-43208)*

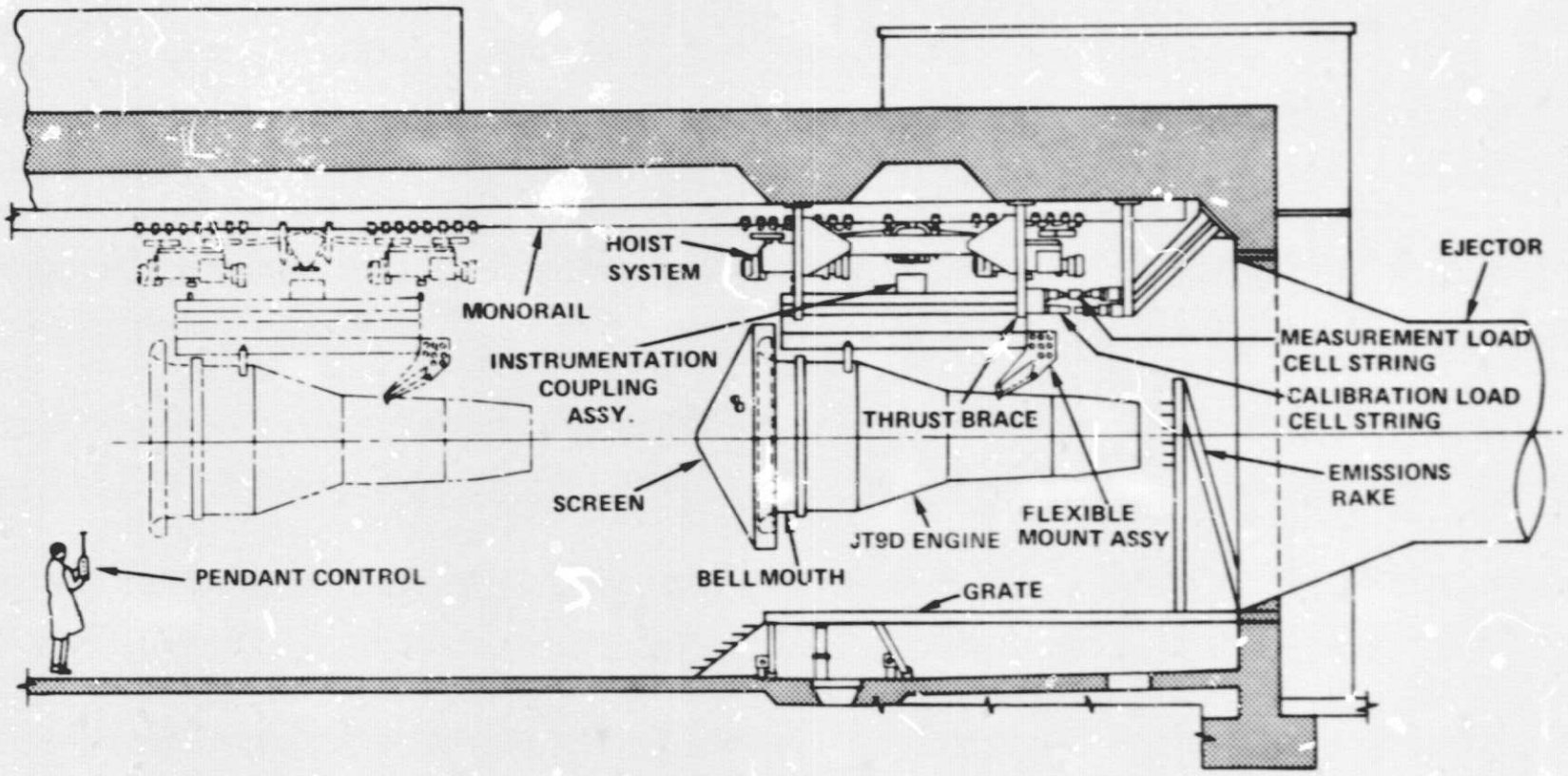


*Figure 3* *P-6 Test Cell Layout*

*Figure 4 Cross Section of Experimental Clean Combustor Program Phase III Vorbix Combustor*

While the two-stage Vorbix burner is a significantly different concept than the current production combustor, since compressor and burner pressure loss are the same as the bill-of-material, the measured turbulence levels in the diffuser should be representative of those in most JT9D-7 engines.

## B. PROBE DESCRIPTION AND LOCATION

Turbulence measurements were conducted at six circumferential and three spanwise positions near the entrance to the diffuser. The locations of the probes are shown in Figure 5. At each circumferential position, the probes were located at 25, 50 or 75 percent span locations. Three types of wire and wedge probes were used during the tests. A summary of the probe locations and types in the three engine tests which were conducted to measure the turbulence in the diffuser is presented in Table I.

The primary devices used in the tests were wedge type probes consisting of an alumina coated platinum thin film sputtered near the leading edge of a quartz wedge (TSI 949K, Thermosystem, Inc.). A line drawing and photograph of this probe are shown in Figures 6a and 6b. A wedge probe located in a probe mounting adaptor is shown in Figure 7. Probes were retracted in the shield during installation and then inserted to a prescribed location determined from prior engine build measurements. The angular orientation of the probes was established by aligning scribe marks of the probes with the engine axis. The probes are insensitive to changes in the angle of attack within ±10 degrees of the mean flow direction.

Two types of wire probes were also used. The probes 370$\mu$ diameter stainless steel or 12$\mu$ diameter Pt-Ir wires were suspended between support posts of a TSI 1226AB probe (Figure 8). These probes were installed in the engine in the same manner as the wedge probes.

Five $P_{T4}$ and five $T_{T4}$ probes were located at the compressor discharge as shown in Figure 5.

## C DATA ACQUISITION SYSTEM

The probes were used with a Thermosystems 1053A anenometer and the signals were recorded with a Hewlett-Packard 3960 magnetic tape recorder with frequency modulated (FM) and direct record and playback modules. Using both FM and direct record modules, it was possible to record data within a 0 to 50 kHz bandwidth. The bandwidth of the data was determined by the transfer function of the probe/lead/anenometer circuit; this transfer function was experimentally determined and used to obtain data within a 0-20 kHz bandwidth (see subsequent section). Since the diffuser turbulence was measured primarily within a 100-5,000 Hz bandwidth, the data acquisition system bandwidth did not limit or affect the turbulence measurements.

Noise levels measured in the engine prior to the test were ~0.9 mV. This electrical noise corresponded to an equivalent input noise turbulent intensity of 0.2 percent at flight idle and reduced to less than 0.1 percent as the engine thrust increased. Data was recorded after a five minute stabilization at each test point. There was no evidence of drift in the turbulence characteristics after the stabilization period.

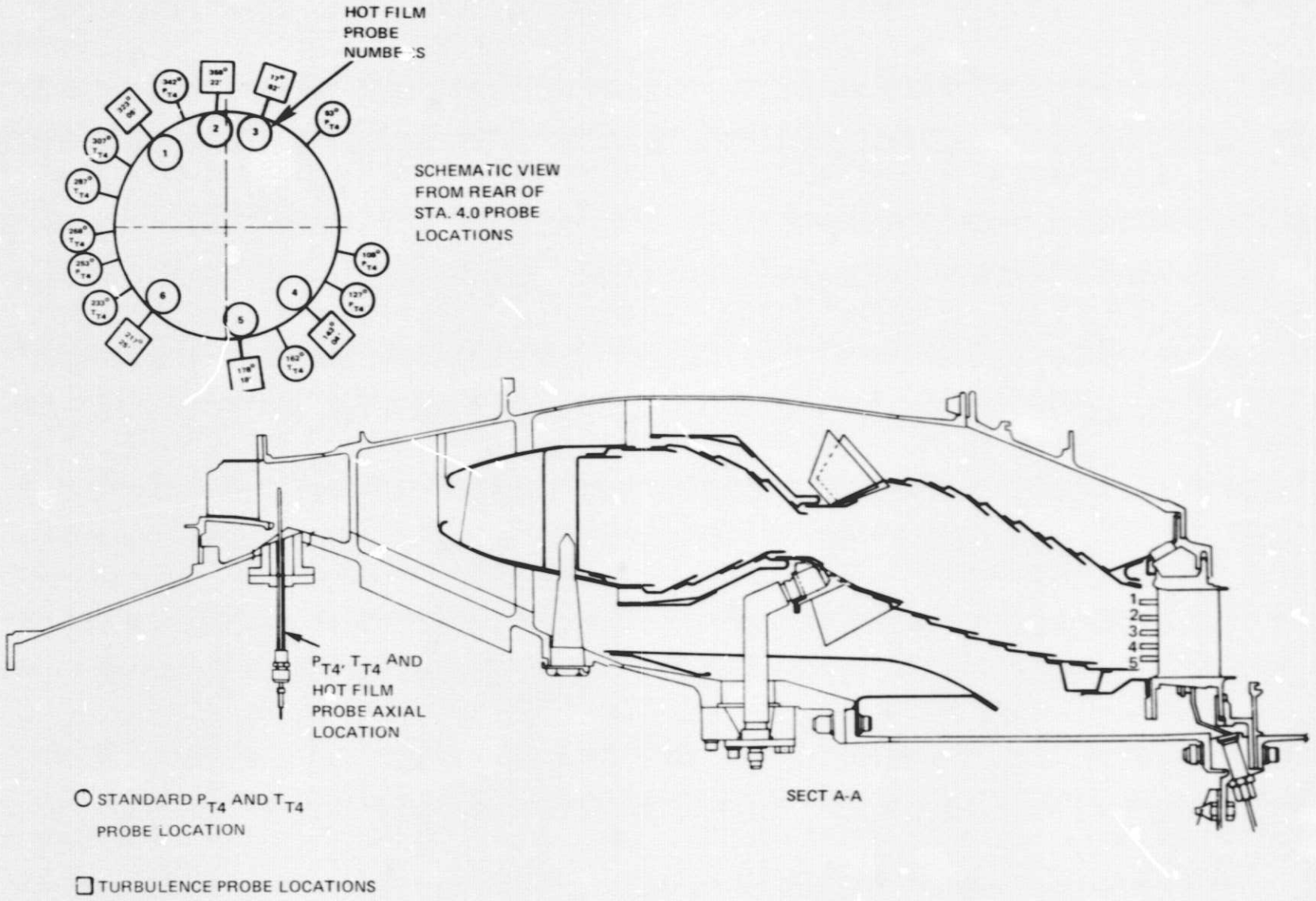


*Figure 5* *Location of Turbulence Probes*

TABLE I

PROBE TYPES AND LOCATIONS

| Test No. 1 *Probe No. | Type | Angular Location | Spanwise Location (Percent) |
|---|---|---|---|
| 1 | 370$\mu$ diameter Stainless Steel Wire Probes | 323° 05′ | 25, 50, 75 |
| 2 | TSI 949K Hot Film Probes | 358° 22′ | 25, 50, 75 |
| 3 | TSI 949K Hot Film Probes | 17° 52′ | 25, 50, 75 |
| 4 | TSI 949K Hot Film Probes | 143° 04′ | 25, 50, 75 |
| 5 | 370$\mu$ diameter Stainless Steel Wire Probes | 178° 18′ | 25, 50, 75 |
| 6 | 12$\mu$ Pt-Ir Wire Probes | 217° 25′ | 25, 50, 75 |

| Test No. 2 *Probe No. | Type | Angular Location | Spanwise Location (Percent) |
|---|---|---|---|
| 1 | 370$\mu$ diameter Stainless Steel Wire Probes | 323° 05′ | 25, 50, 75 |
| 2 | 370$\mu$ diameter Stainless Steel Wire Probes | 358° 22′ | 25, 50, 75 |
| 3 | 370$\mu$ diameter Stainless Steel Wire Probes | 17° 52′ | 25, 50, 75 |
| 4 | | | |
| 5 | 370$\mu$ diameter Stainless Steel Wire Probes | 178° 18′ | 25, 50, 75 |
| 6 | 12$\mu$ Pt - Ir Wire Probes | 217° 25′ | 25, 50, 75 |

| Test No. 2 *Probe No. | Type | Angular Location | Spanwise Location (Percent) |
|---|---|---|---|
| 1 | TSI 949K Hot Film Probe | 323° 05′ | 25, 50, 75 |
| 2 | TSI 949K Hot Film Probe | 358° 22′ | 25, 50, 75 |
| 3 | TSI 949K Hot Film Probe | 17° 52′ | 25, 50, 75 |
| 4 | TSI 949K Hot Film Probe | 143° 04′ | 25, 50, 75 |
| 5 | TSI 949K Hot Film Probe | 178° 18′ | 25, 50, 75 |
| 6 | TSI 949K Hot Film Probe | 217° 25′ | 25, 50, 75 |

*See Figure 5 for Probe Location

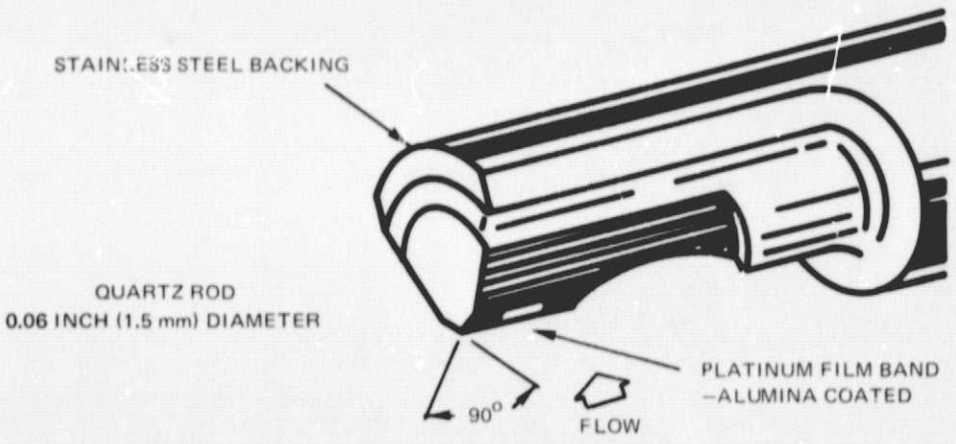


SENSING SIZE: TWO WEDGE SURFACES EACH 0.005 INCH (0.12 mm) WIDE BY 0.04 INCH (1.0 mm) LONG

**(a)**

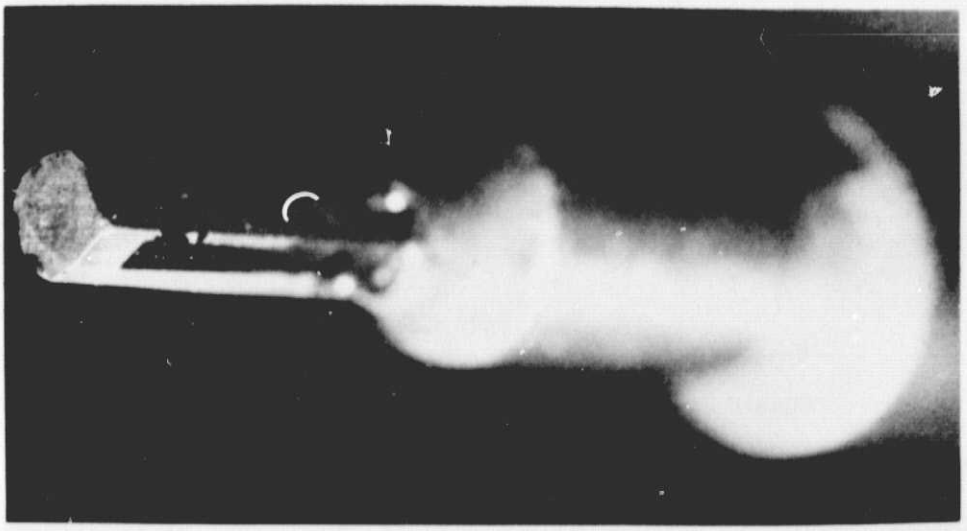

**(b)**

*Figure 6 Wedge Type Probe (77-444-9004)*

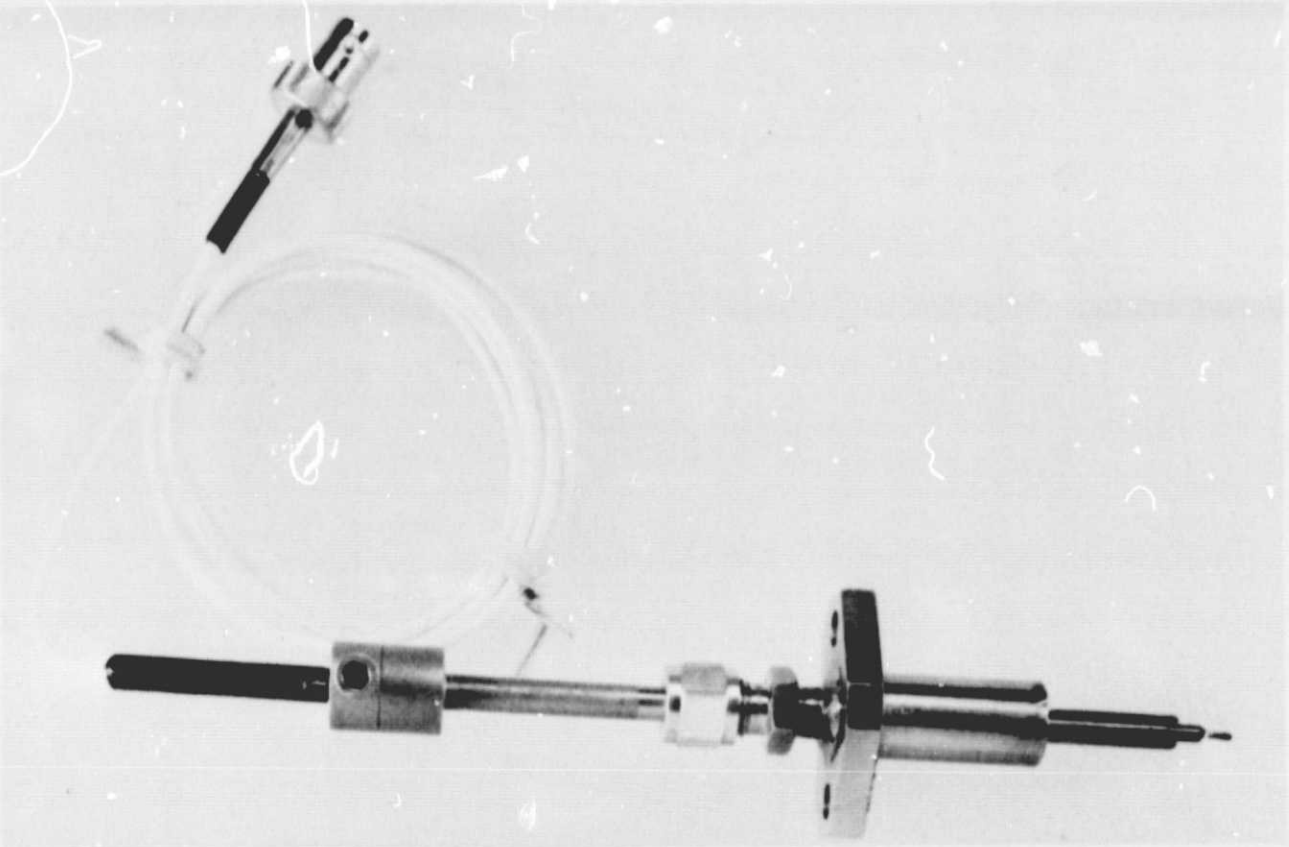

*Figure 7* *Station 4 Probe Adaptor* *(77-441-9142)*

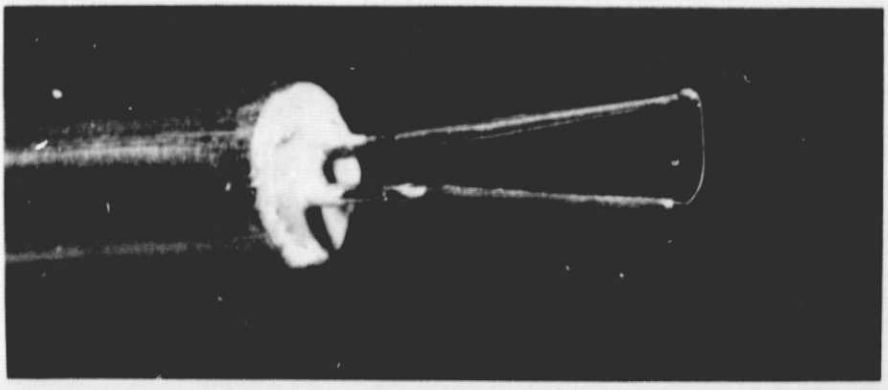

*Figure 8* *Wire Probe* *(77-444-9002A)*

## D. CALIBRATION PROCEDURES

The probes were subjected to a series of calibrations procedures prior to use in an engine test. The stability of the wedge probes was checked by heating the probes to 516K for approximately 30 minutes and measuring the changes in the film resistivity. Irreversible resistance changes of the probes used in the engine tests were found to be less than 0.2 percent. Typical resistances of the probes between 297K and 589K are shown in Figure 9.

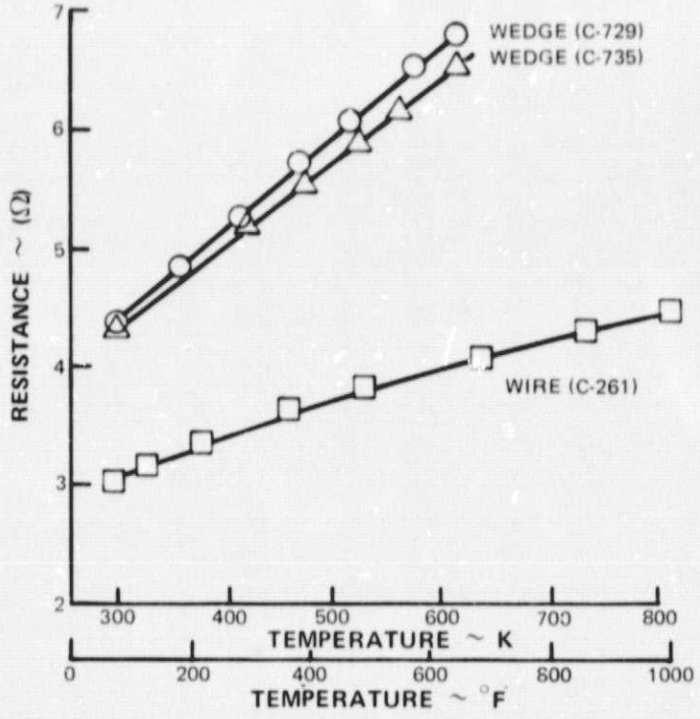


*Figure 9 Dependence of Probe Resistance on Temperature*

The heat transfer to a probe in a gas stream is described by the one dimensional heat balance equation at the surface of the probe,

$$hA\,(T - T_G) = \frac{R}{(R + R_b)^2}\,(E^2 - E_C{}^2) \qquad (1)$$

where $h$ = heat transfer coefficient, $KW/m^2K$

$A$ = surface area, $m^2$

$T$ = average surface temperature, K

$T_G$ = average gas temperature, K

$R$ = sensor resistance, $\Omega$

$R_b$ = resistance of resistor in series with sensor in anenometer circuit, $\Omega$

$E$ = bridge voltage in test environment, V,

and, $E_C$ = bridge voltage in quiescent environment, V.

In equation 1 the left side represents the heat liberated due to convection and the right side is the heat liberated due to joulian heating. The convection heat transfer coefficient is specified by the velocity, temperature, and pressure of the environment; the general relationship is written

$$h = Ku^n$$

where $K = K[P,T]$

Substituting this expression into equation 1 and simplifying yields:

$$u^n = C[E^2 - E_C{}^2] \qquad (2)$$

where $$C = \frac{R}{KA(T - T_G)(R + R_b)^2}$$

The velocity, u, and bridge voltage, E, can be separated into the steady state and wide bandwidth components, giving

$$u = \bar{u} + \tilde{u} = \bar{u}\left(1 + \frac{\tilde{u}}{\bar{u}}\right)$$

and,

$$E = \bar{E} + \tilde{E} = \bar{E}\left(1 + \frac{\tilde{E}}{\bar{E}}\right)$$

Assuming $\tilde{u}/\bar{u} << 1$ and $\tilde{E}/\bar{E} << 1$ the following simplifications apply:

$$u^n = [\bar{u}(1 + \frac{\tilde{u}}{\bar{u}})]^n \approx \bar{u}^n \left(1 + n\frac{\tilde{u}}{\bar{u}}\right)$$

and,

$$E^2 = \bar{E}^2\left(1 + 2\frac{\tilde{E}}{\bar{E}}\right)$$

Substituting these approximations into equation 2 and simplifying yields an expression for the average velocity, u, and the turbulent intensity, $\tilde{u}/\bar{u}$, written

$$u = [C(E^2 - E_C{}^2)]^{1/n}$$

and (3)

$$\frac{\tilde{u}}{\bar{u}} = \frac{2}{n}\left(\frac{\tilde{E}\,\bar{E}}{\bar{E}^2 - E_C{}^2}\right)$$

Probe calibration consisted of determining the values of n and $E_C$ for use in equation 3. $E_C$ values are measured separately in a laboratory furnace. Examples of the dependence of $E_C$ on the temperature of wedge and stainless steel wire probes are shown in Figure 10.

Taking the log of both sides of equation 2 yields

$$\log (E^2 - E_C^2) = n \log u - \log c$$

A log-log plot of $(E^2 - E_C^2)$ versus u values measured in a known velocity gas stream gives a straight line with constant slope. Although the value of C varies with temperature, pressure and overheat, $\Delta T$, (where $\Delta T$ is defined as $T-T_G$), the slope remains constant. Therefore, ambient conditions are used for this calibration procedure. The experimental arrangement for determining the dependence of the probe voltage $(E^2 - E_C^2)$, on the mean velocity of a cold jet is shown in Figure 11. Example $(E^2 - E_C^2)$ vs. u curves are presented in Figure 12 where it is seen that the slope for a given probe is indeed constant over the experimental range of velocities.

The transfer functions of the probes also were determined in the cold jet. The output of the probes was compared with the output of a 6$\mu$ platinum wire probe which had a flat response over the bandwidth of interest. An example transfer function of a wedge probe is presented in Figure 13. These transfer functions were not found to be a strong function of Reynolds number.

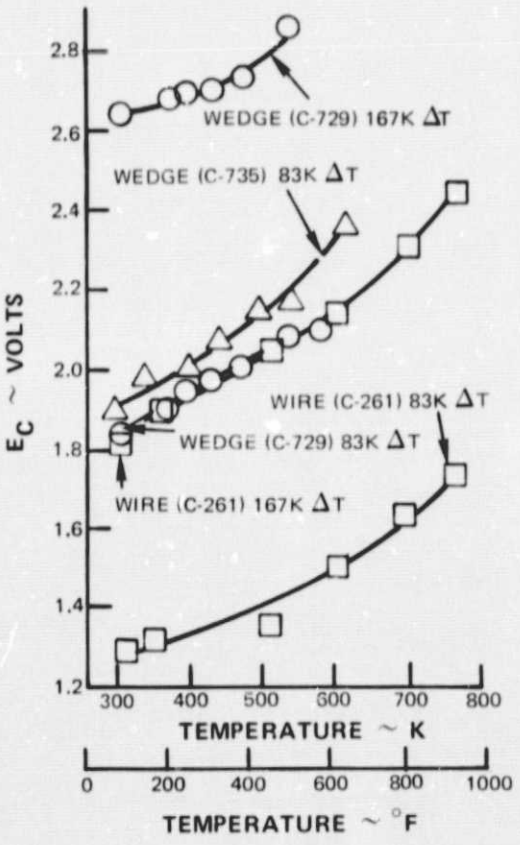


*Figure 10* *Dependence of Quiescent Environment Bridge Voltage On Temperature*

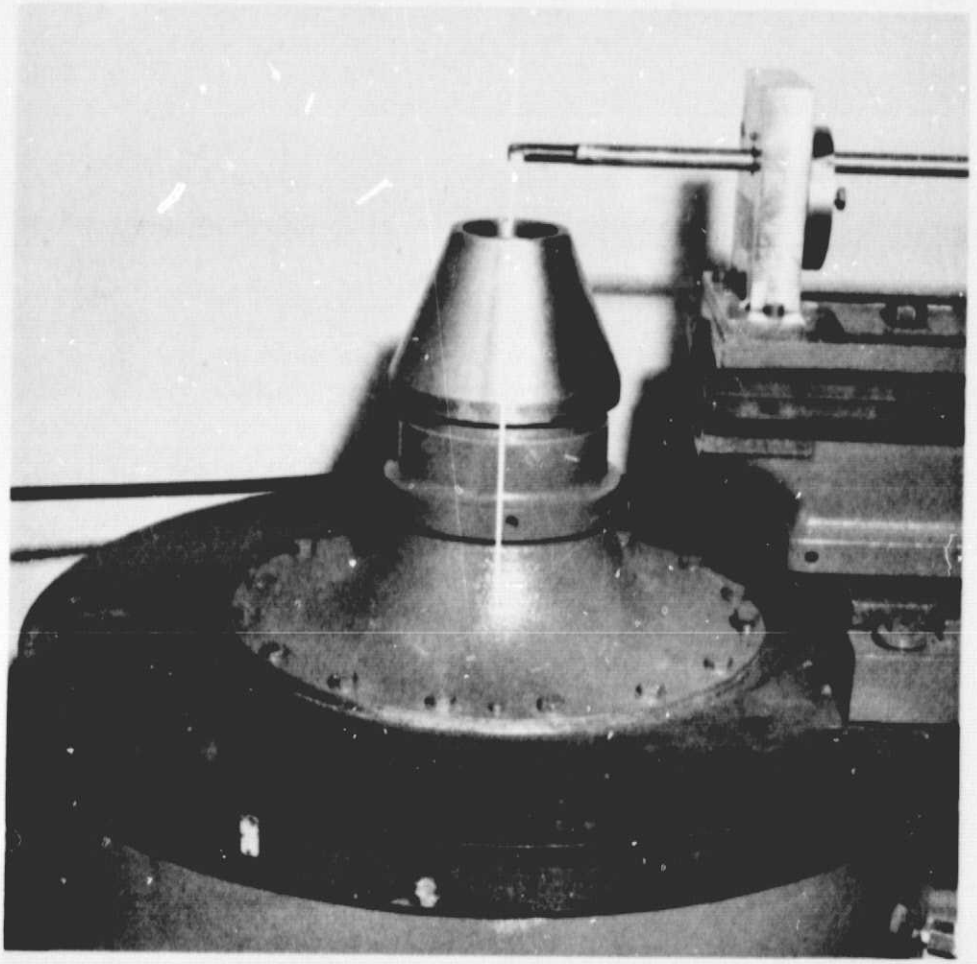

*Figure 11* *Experimental Arrangement for Anemometer Velocity Calibrations* *(X-30941)*

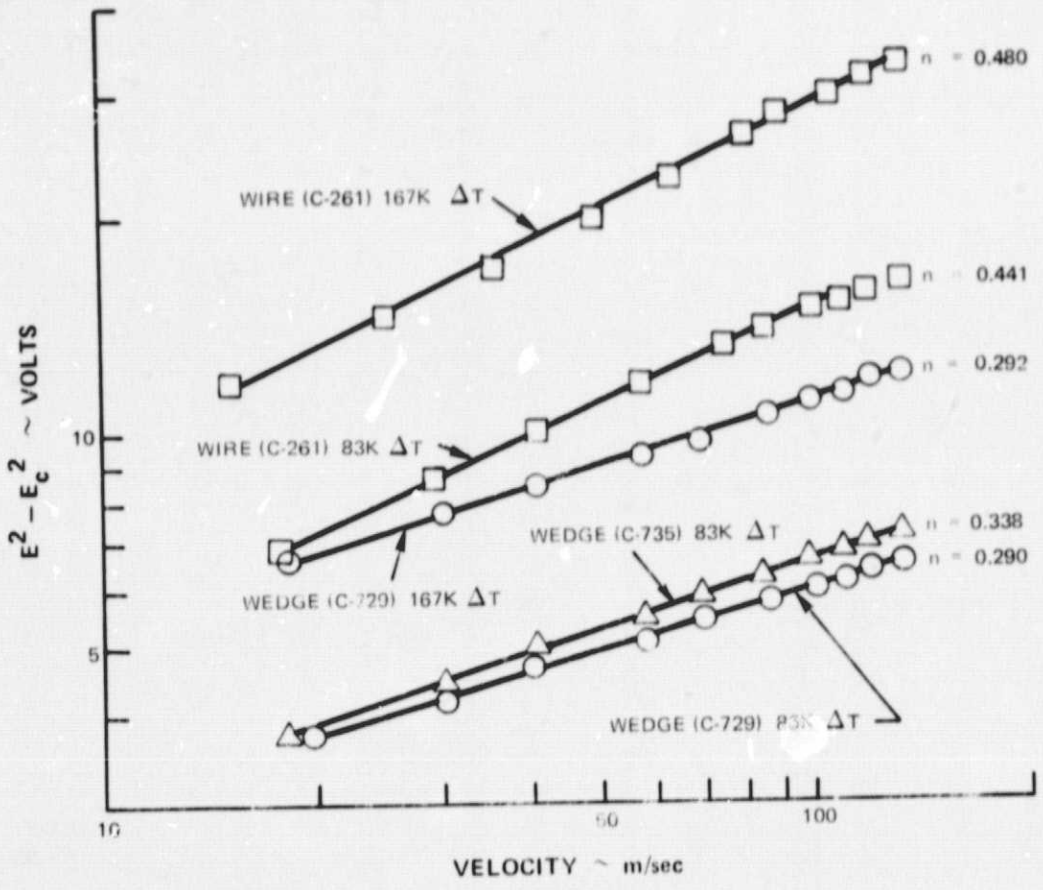


*Figure 12 Anemometry Probe Velocity Calibrations*

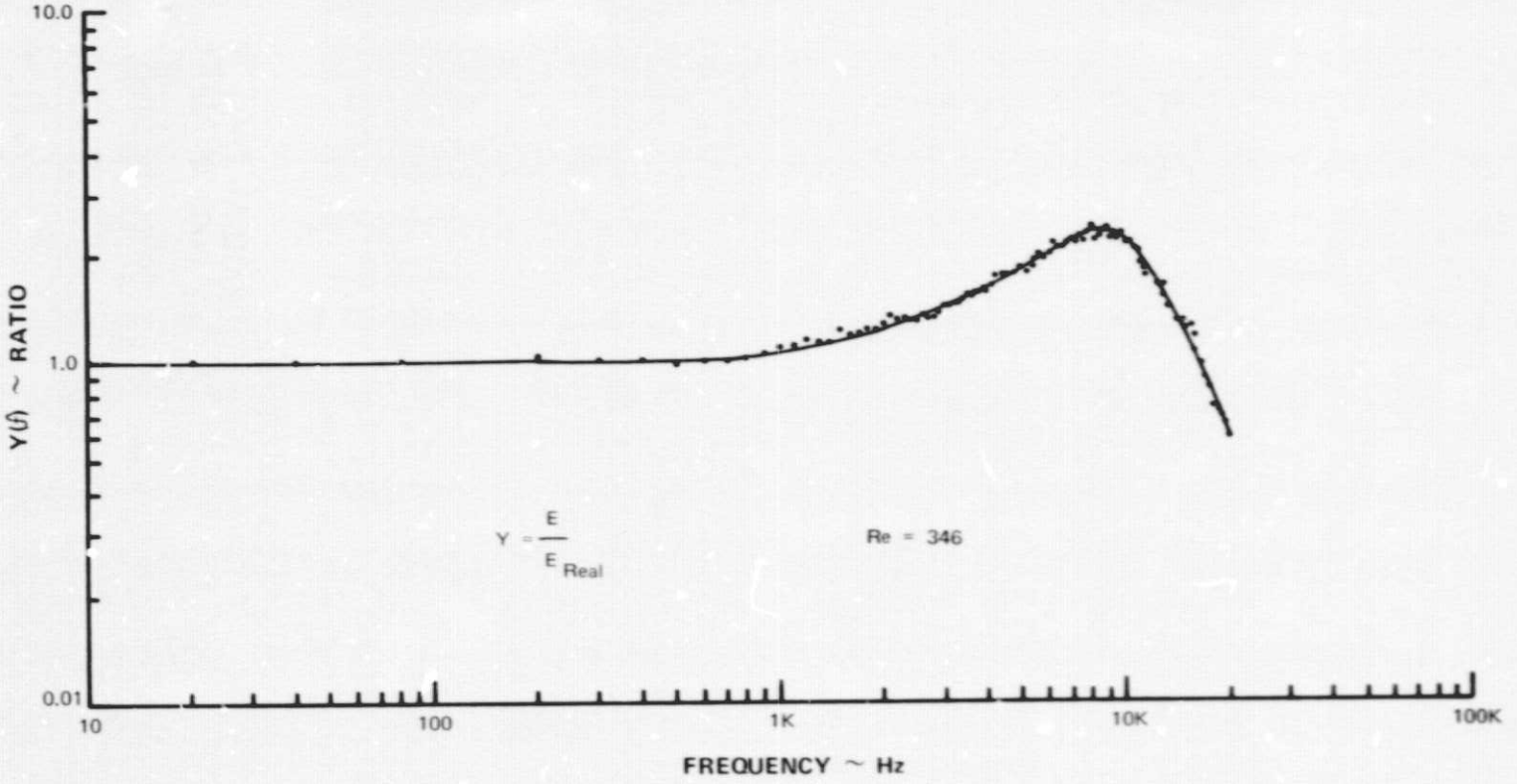


*Figure 13* *Wedge Probe Transfer Function*

## E. DATA REDUCTION PROCEDURES

The properties of turbulence of most interest to the engine designer and analyst are (a) the total kinetic energy of the longitudinal turbulent fluctuations (proportional to turbulence intensity or mean deviation of the velocity; i.e., to $\sqrt{\overline{u'^2}}/\bar{u}$ where u is the instantaneous magnitude of the velocity component in the streamwise direction), (b) the integral scale $\Lambda$ (which is the average size of all turbulent eddies, a measure of mixing length), (c) the microscale $\lambda$ (which is the average size of the smallest eddies, where viscous energy dissipation to heat takes place), and (d) the frequency spectrum of the turbulent velocity fluctuations (revealing the presence or absence of any strong disturbances at discrete frequencies). If the turbulence intensity is below 0.10 and if the frequency spectrum is relatively smooth and featureless, then only classical free turbulence is present (generated by wakes and wall friction effects far upstream). In this type of turbulence the calculation of $\sqrt{\overline{u^2}}$, $\lambda$, $\Lambda$ are straight forward [Reference 2] and the interpretation clear. If the intensity is above 0.1 or the spectrum contains peaks, then phenomena other than classical free turbulence are present (e.g. wall stall, discrete vortex streets, plug flow oscillations, or other non-random mechanisms.)

These features of the velocity waves were determined from the recorded signals. First, the data were analyzed with a spectrum analyzer (Federal Scientific Model UA 500) to obtain the individual fourier components of the waves. Due to the nature of the turbulence, it was found that a full scale analyzer range of 20,000 Hz was sufficient to include all the fourier components of the turbulence. The data in the range 50 Hz to 20,000 Hz were separated into 399 components of 50 Hz bandwidth. The data was averaged for 25 seconds to obtain accurate values of the fourier coefficients.

The 399 channels of information were transferred to a PDP-11/40 mini-computer where each value was corrected for the gains or attenuations encountered during amplification, recording, and spectral analysis. The signals were also adjusted to compensate for the experimental values of the transfer function (Y(f), according to the relation

$$E_R(f) = \frac{1}{A_e} \cdot \frac{E(f)}{Y(f)}$$

where $E_R(f)$ = corrected anemometer voltage V

$E(f)$ = anemometer voltage measured with the spectrum analyzer

$Y(f)$ = anemometer transfer function

$A_e$ = sum of gains and attenuations in the data recording and analysis circuits

The Power Spectral Density function, PSD (f), defined as

$$PSD(f) = \frac{\overline{\tilde{u}(f)^2}}{b} \qquad (4)$$

where a superscript bar indicates a time-averaged quantity and where b is the bandwidth per channel, was computed from a combination of equations 3 and 4.

$$PSD(f) = \frac{\left[\overline{\left[\frac{\tilde{u}(f)}{\bar{u}}\right]^2}\right](\bar{u})^2}{b} \qquad (5)$$

$$= \frac{\left[\overline{\tilde{E}_R(f)}\right]^2}{b} \left[\frac{2}{n} \frac{\bar{E}\,\bar{u}}{(\bar{E}^2 - E_C{}^2)}\right]^2 \frac{(m/sec)^2}{Hz}$$

Where, $\bar{E}$ was determined by measuring the average D.C. voltage recorded on the FM channel. The average velocity, $\bar{u}$ was estimated from a conservation of mass analysis at the axial location of the sensors. The values of n and $E_C$ were obtained from the probe calibrations conducted prior to the engine test. The individual PSD components were plotted as a function of frequency. The RMS value of the turbulence, Tu, or the power distribution function, $\overline{PSD}$, is defined as

$$Tu = \sqrt{\int_{f_1}^{f_n} \left[\frac{\overline{\tilde{u}(f)}}{b}\right]^2 df}$$

where $f_n$ and $f_1$ are the upper and lower limits of the frequency range of interest, or

$$\overline{PSD} = \sqrt{\int_{f_1}^{f_n} PSD(f)\, df}$$

where $Tu \equiv \overline{PSD}$

The turbulence intensity is defined as $Tu/\bar{u}$

The power distribution function was computed from the 399 samples of data at 50 Hz bandwidth, using the summation

$$\overline{PSD} = \sqrt{50 \sum_{i=1}^{n} PSD\ (f_i)}$$

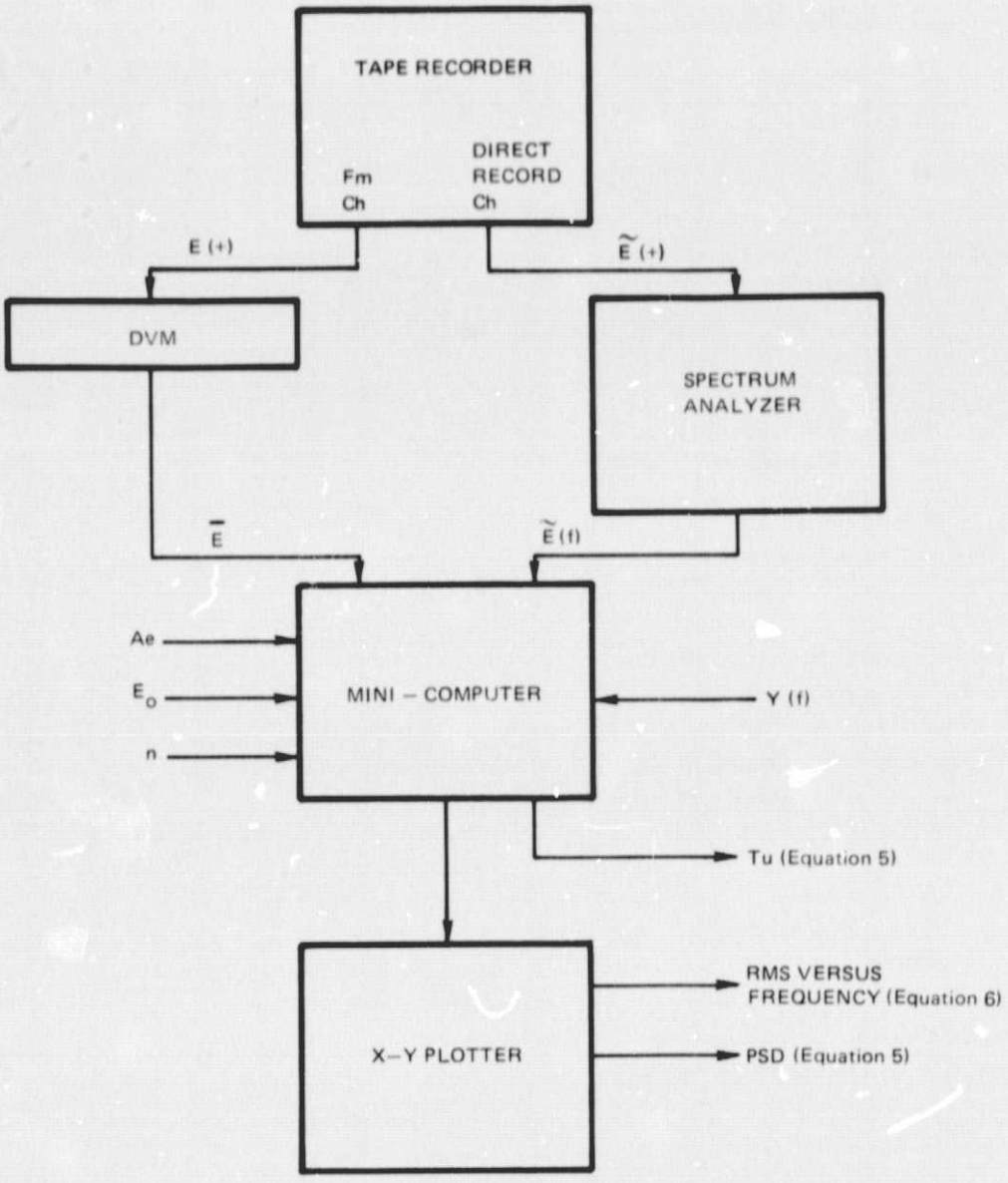


*Figure 14* *Block Diagram of Data Reduction System*

Microscale and macroscale were calculated from the power spectral density curves using the classical definitions [Reference 2].

$$\text{Macroscale} \quad \Lambda = \frac{\bar{u}}{4} \quad \frac{[\text{PSD}\ (100)]}{\overline{u^2}} \tag{7}$$

$$\text{Microscale} \quad \lambda = \frac{1}{\sqrt{2}\,\pi} \quad \frac{\bar{u}\,Tu}{\sqrt{\int f^2\ [\text{PSD}\ (f)]\ df}} \tag{8}$$

where $\bar{u}$ = mean velocity

$Tu$ = rms turbulence level

$f$ = frequency (Hz)

PSD (f) = power spectral density function. [PSD (f)] df is the contribution to $(\widetilde{u})^2$ of the frequencies between f and f + df.

The minicomputer in the block diagram of Figure 14 provided the means to accomplish this standard calculation, since all the quantities of equations (7) and (8) were already available in the minicomputer. This procedure is exactly equivalent to that used in Reference 3 in which analog signals proportional to u and du/dt are processed as follows:

a) $\lambda = u \left[\sqrt{\bar{u}^{\,2}} / \sqrt{\overline{du/dt}^2}\right]$

b) $\Lambda$ is obtained by playing the tape into an autocorrelator to obtain a plot of autocorrelation versus time delay ($\tau$). The integral scale is equal to the time delay at which autocorrelation vanishes ($\tau_o$) multiplied by stream velocity (u).

The availability of the minicomputer and the use of equations (7) and (8) provided better accuracy (less reprocessing of raw analog signals).

## CHAPTER II

## RESULTS AND DISCUSSION

Three engine tests were conducted to measure the turbulence levels in the diffuser. A summary of the test points is presented in Tables II through IV with the diffuser duct temperature. A complete description of the engine and diffuser performance parameters is presented in Table V. As seen in Table II, all three types of probes were used in Test 1. Probes 1 and 6 failed immediately at the first idle point. Probe 5 remained partially intact, although it was damaged and provided erratic and aphysical data; the probe failed completely at the first approach point. Probe 4 also generated erratic data which was not reproducible when the engine was returned to idle. The problem appeared to be due to a ground loop.

Probes 2 and 3 provided reliable data throughout the engine test; a summary of the turbulent intensities are presented in Table II. While the probe 3 data was more reproducible at idle than the probe 2 data, both sets of data are in reasonable agreement. There appears to be a gradual increase in the turbulent intensity with engine thrust.

The diffuser gas temperature in Test 1 was limited to 616 K, the maximum operating temperature of the wedge probes. In Test 2, the stainless steel and Pt-IR wire probes were used in an attempt to obtain data above 616 K $T_{T4}$. The anemometers were set for operation at a climb $T_{T4}$ of 736 K and the engine was started, idled for 5 minutes and immediately accelerated to the climb test point. Probe 6 (Pt-Ir) was destroyed during installation; the remaining probes were intact after the idle engine equilibration. Probes 1, 2 and 3 broke during acceleration to the climb test point. At the climb test point, probe 5 failed and the test was terminated.

Test 3 was more successful. Six wedge probes were used to obtain turbulence data from idle ($T_{T4} \approx 450$ K) to approach ($T_{T4} \approx 616$ K). Probes 3 and 5 were unstable, apparently due to intermitent connections at the probe, but the remaining probes provided reliable, reproducible test data during the entire engine test.

At the 25 percent span position, the data are in agreement with the initial data; again, there appears to be a gradual increase in the turbulence with engine thrust. The turbulent intensity is not a strong function of the engine thrust. At the 75 percent span position, the turbulence level is higher at each test point and shows a much more marked dependence on the engine thrust level (Figure 15). The approach value of ~ 15 percent was unexpected.

The PSD functions of the velocity waves measured at all the locations and engine operation levels except for blade passing frequency were quite featureless. Example PSD functions at the 25 percent and 75 percent span location at idle and approach are shown in Figures 16 through 19. The corresponding PSD functions are shown in Figures 20 through 23. Over the entire operating range of measurements, the PSD functions were flat with a cutoff (−3 dB) frequency of approximately 3 kHz. The cutoff frequency was not a function of the engine thrust. Above 3 kHz, the PSD function is proportional to $f^{-5 \pm 0.2}$; the amplitude of the velocity fourier components decays at a rate proportional to $f^{-2.5 \pm 0.1}$. Approximately 95 percent of the power in the velocity waves is contained in frequency components below 5 kHz.

## TABLE II

DEPENDENCE OF TURBULENT INTENSITY ON ENGINE OPERATION, TEST 1

| Test Point | Designation | Probe 1 S.S. Wire 323° 5′ 50% Span | | Probe 2 Hot Film 358° 22′ 50% Span | | Probe 3 Hot Film 17° 52′ 25% Span | | Probe 4 Hot Film 143° 04′ 75% Span | | Probe 5 S.S. Wire 178° 18′ 50% Span | | Probe 6 Pt.-Ir. Wire 217° 25′ 50% Span | |
|---|---|---|---|---|---|---|---|---|---|---|---|---|---|
| | | $T_4$ K | $Tu/\bar{u}$ % | $T_4$ K | $Tu/\bar{u}$ % | $T_4$ K | $Tu/\bar{u}$ % | $T_4$ K | $Tu/\bar{u}$ % | $T_4$ K | $Tu/\bar{u}$ % | $T_4$ K | $Tu/\bar{u}$ % |
| 1 | Idle | Failed | | 450 | 7.0 | 454 | 4.76 | Erratic | | Erratic | | Failed | |
| 2 | Flight Idle | Failed | | 516 | 8.16 | Erratic | | Erratic | | Erratic | | Failed | |
| 3 | Approach | Failed | | 591 | 7.64 | 597 | 6.65 | Erratic | | Erratic | | Failed | |
| 4 | Idle | Failed | | 456 | 6.59 | 464 | 4.78 | Erratic | | Failed | | Failed | |
| 5 | Rich Approach | Failed | | 608 | 7.96 | 616 | 5.42 | Erratic | | Failed | | Failed | |
| 6 | Idle | Failed | | 455 | 5.22 | 455 | 4.81 | Erratic | | Failed | | Failed | |

## TABLE III

DEPENDENCE OF TURBULENT INTENSITY ON ENGINE OPERATION, TEST 2

| Test Point | Designation | Probe 1 S.S. Wire 323° 05′ 25% Span | | Probe 2 S.S. Wire 358° 22′ 75% Span | | Probe 3 S.S. Wire 17° 52′ 50% Span | | Probe 4 None Installed | | Probe 5 S.S. Wire 178° 18′ 50% Span | | Probe 6 Pt-Ir Wire 217° 25′ 25% Span | |
|---|---|---|---|---|---|---|---|---|---|---|---|---|---|
| | | $T_4$ K | $Tu/\bar{u}$ % | $T_4$ K | $Tu/\bar{u}$ % | $T_4$ K | $Tu/\bar{u}$ % | $T_4$ K | $Tu/\bar{u}$ % | $T_4$ K | $Tu/\bar{u}$ % | $T_4$ K | $Tu/\bar{u}$ % |
| 1 | Climb | Failed | | Failed | | Failed | | – | – | Erratic | | Failed | |

## TABLE IV

### DEPENDENCE OF TURBULENT INTENSITY ON ENGINE OPERATION, TEST 3

| Test Point | Designation | Probe 1 Hot Film 323° 05′ 25% Span | | Probe 2 Hot Film 358° 22′ 75% Span | | Probe 3 Hot Film 17° 52′ 50% Span | | Probe 4 Hot Film 143° 4′ 75% Span | | Probe 5 Hot Film 178° 18′ 50% Span | | Probe 6 Hot Film 217° 25′ 25% Span | |
|---|---|---|---|---|---|---|---|---|---|---|---|---|---|
| | | $T_4$ K | $Tu/\bar{u}$ % | $T_4$ K | $Tu/\bar{u}$ % | $T_4$ K | $Tu/\bar{u}$ % | $T_4$ K | $Tu/\bar{u}$ % | $T_4$ K | $Tu/\bar{u}$ % | $T_4$ K | $Tu/\bar{u}$ % |
| 1 | Idle | 461 | 6.83 | 452 | 7.09 | Erratic | | 450 | 7.93 | Erratic | | 459 | 5.87 |
| 2 | Flight Idle | 536 | 7.70 | 525 | 10.56 | Erratic | | 520 | 11.03 | Erratic | | 519 | 6.14 |
| 3 | Approach | 611 | 7.09 | 602 | 16.17 | Erratic | | 597 | 14.17 | Erratic | | 602 | 5.68 |
| 4 | Idle | 461 | 6.88 | 453 | 7.05 | Erratic | | 447 | 8.08 | Erratic | | 452 | 6.18 |

## TABLE V

### ENGINE TEST CONDITIONS

| | Test Pt. | Designation | $T_{T4}$* K | $P_{T4}$* $10^5$ N/m$^2$ | Average Velocity Calculated From $P_{T4}/T_{T4}$ m/sec | F/A | $N_2$ RPM | Fn N |
|---|---|---|---|---|---|---|---|---|
| Test 1 | 1 | Idle | 450 | 3.71 | 109.3 | 0.0096 | 4941 | 14052 |
| | 2 | Flight Idle | 520 | 6.02 | 112.2 | 0.0106 | 5765 | 31471 |
| | 3 | Approach | 590 | 9.17 | 122.8 | 0.0140 | 6376 | 61759 |
| | 4 | Idle | 452 | 3.76 | 108.9 | 0.0095 | 4983 | 14470 |
| | 5 | Rich Approach | 609 | 9.91 | 128.1 | 0.0148 | 6499 | 70366 |
| | 6 | Idle | 446 | 3.63 | 107.1 | 0.0095 | 4913 | 13549 |
| Test 2 | 1 | Climb | 732 | 18.2 | 139.3 | 0.0227 | 7206 | 169030 |
| Test 3 | 1 | Idle | 454 | 3.88 | 110.1 | 0.0102 | 4830 | 16436 |
| | 2 | Flight Idle | 520 | 6.16 | 119.2 | 0.0118 | 5557 | 35177 |
| | 3 | Approach | 599 | 9.77 | 125.7 | 0.0152 | 6203 | 72284 |
| | 4 | Idle | 449 | 3.80 | 122.1 | 0.0103 | 4801 | 16018 |

*Measured

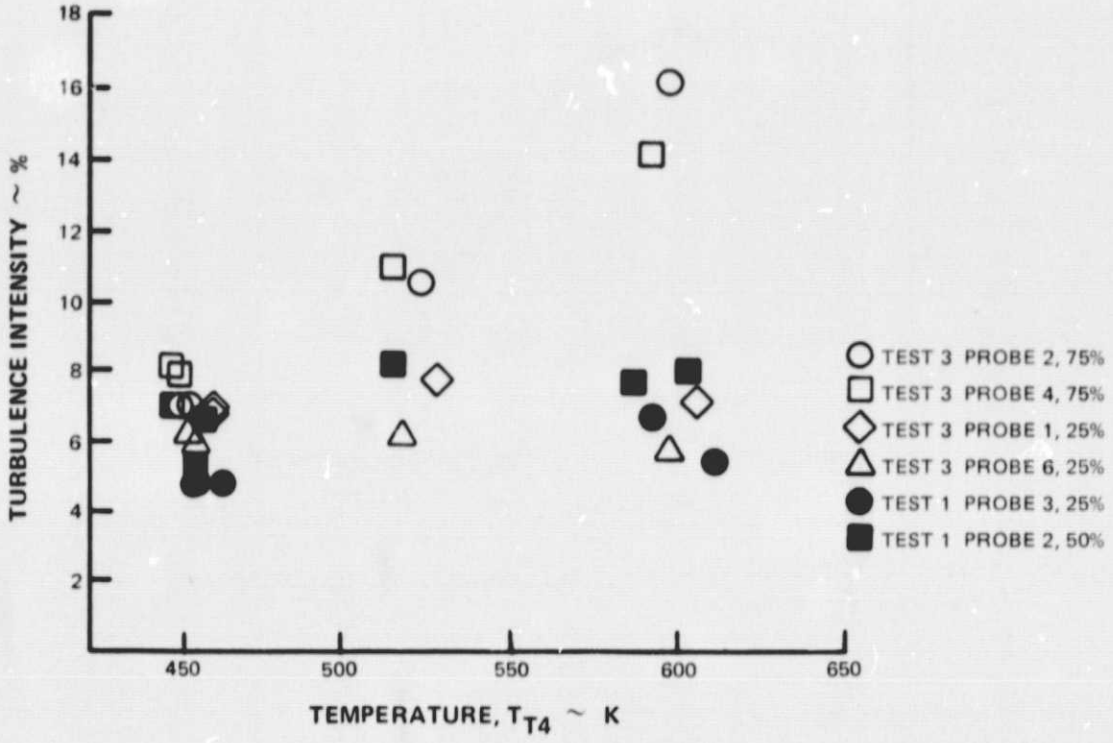


*Figure 15* *Dependence of Turbulence on Engine Operation*

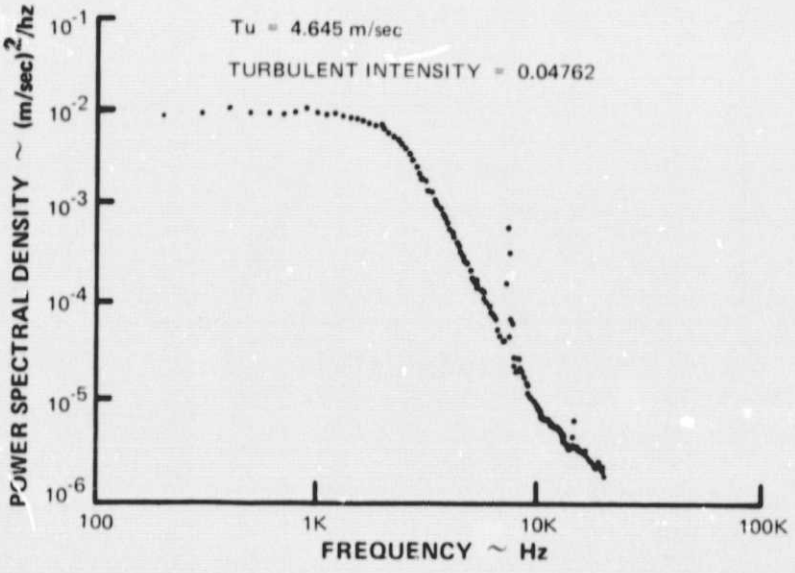


*Figure 16* *Test 1, Probe 3 (Wedge Type) Power Spectral Density Function for Idle Condition at 25 Percent Span*

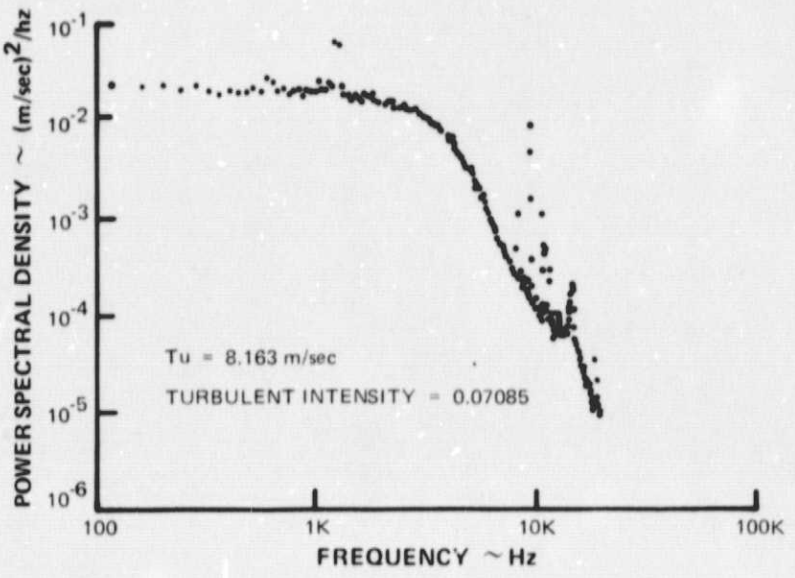


*Figure 17* *Test 3, Probe 1 (Wedge Type) Power Spectral Density Function for Approach Power Condition at 25 Percent Span*

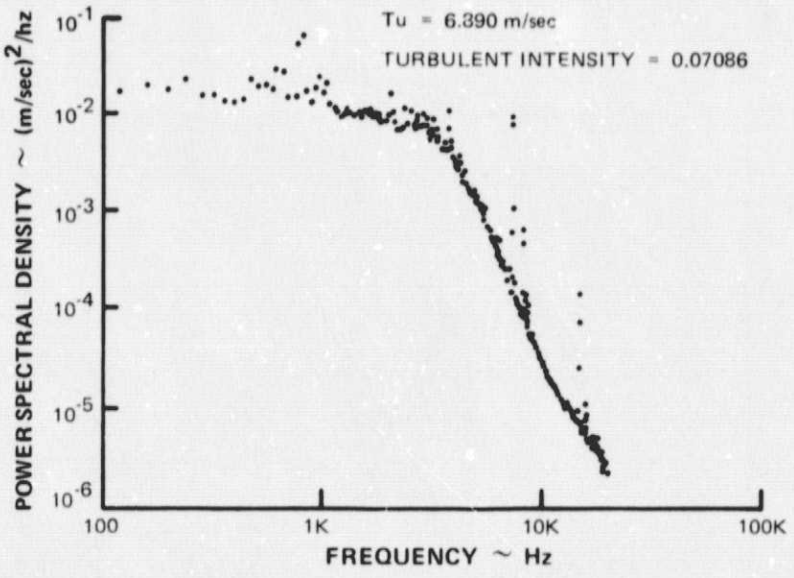


*Figure 18* *Test 3, Probe 2 (Wedge Type) Power Spectral Density Function for Idle Condition at 75 Percent Span*

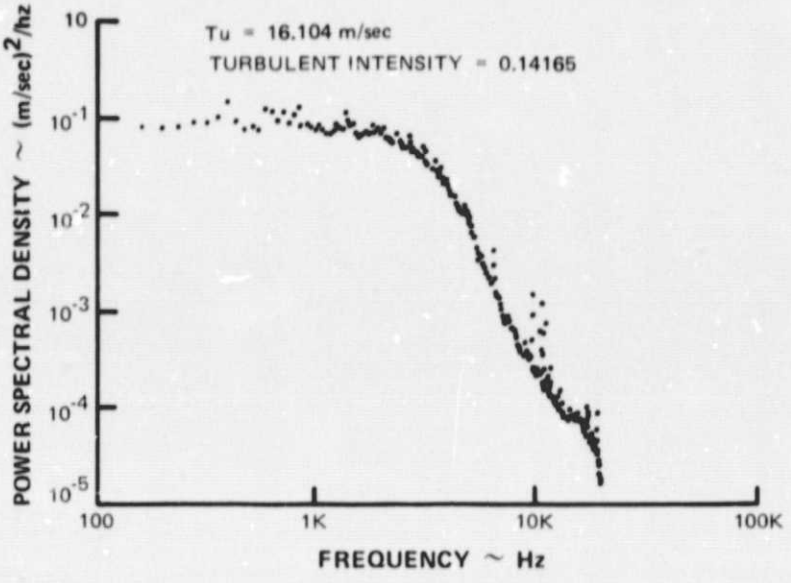


*Figure 19* *Test 3, Probe 4 (Wedge Type) Power Spectral Density Function for Approach Power Condition at 75 Percent Span*

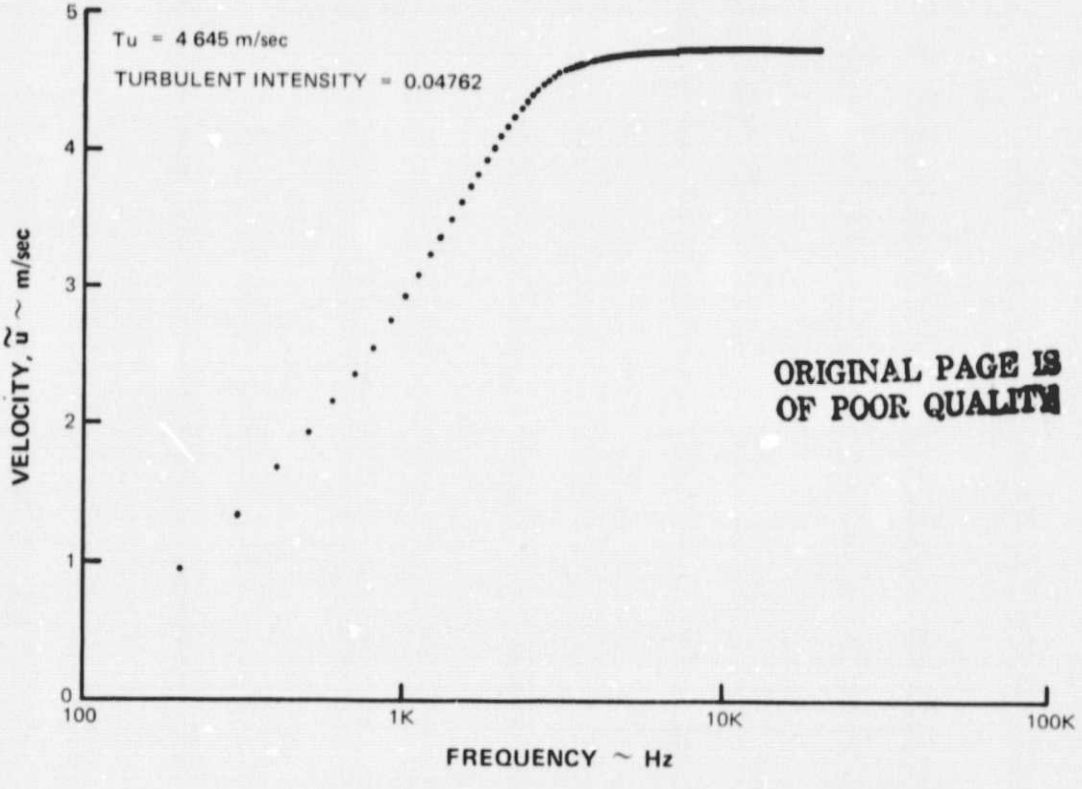




*Figure 20* *Test 1, Probe 3 (Wedge Type) Spectral Distribution for Idle Condition at 25 Percent Span*

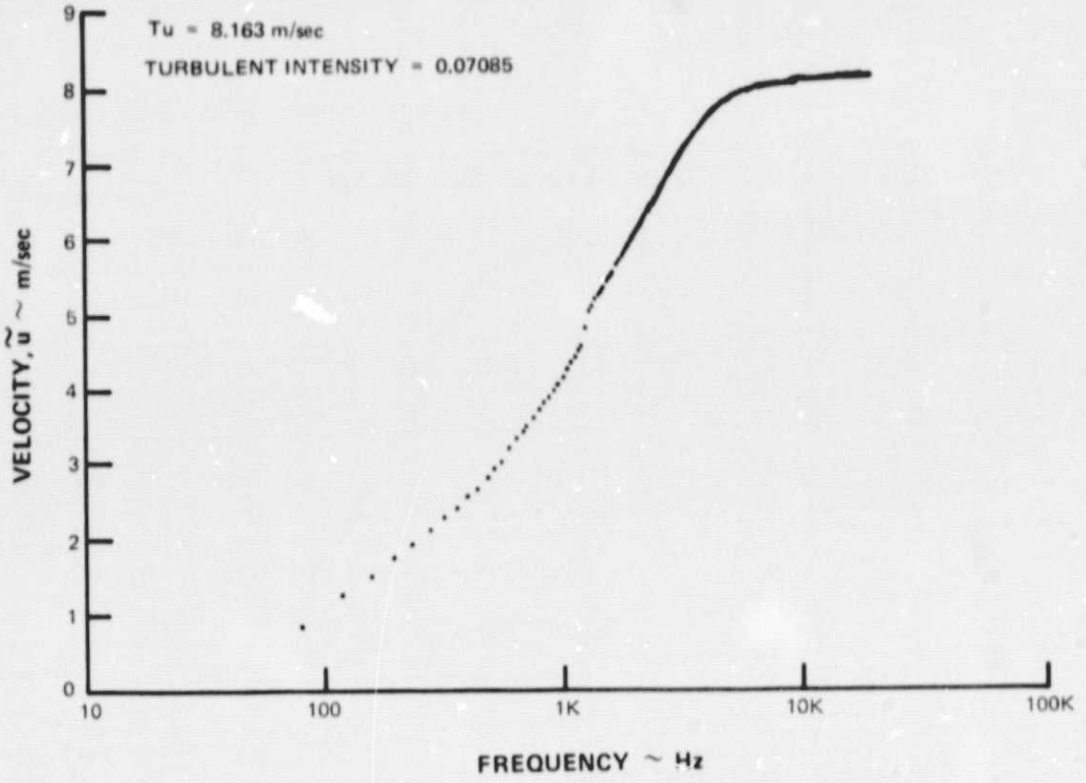


*Figure 21* *Test 3, Probe 1 (Wedge Type) Spectral Distribution for Idle Condition at 25 Percent Span*

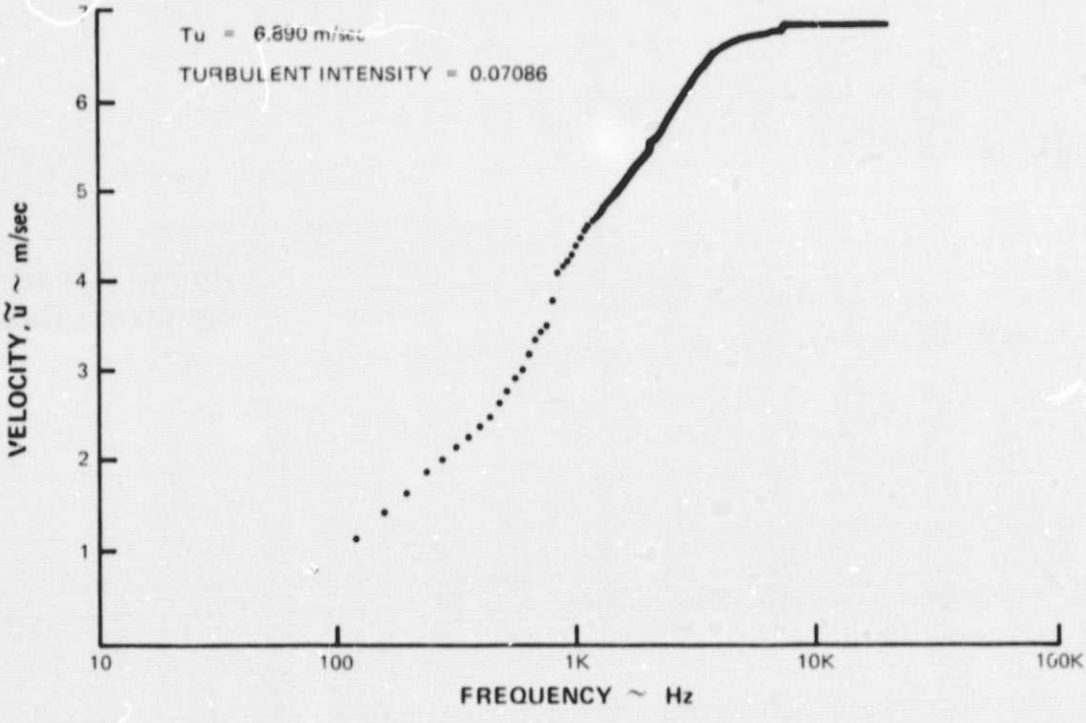


*Figure 22* *Test 3, Probe 2 (Wedge Type) Spectral Distribution for Idle Condition at 75 Percent Span*

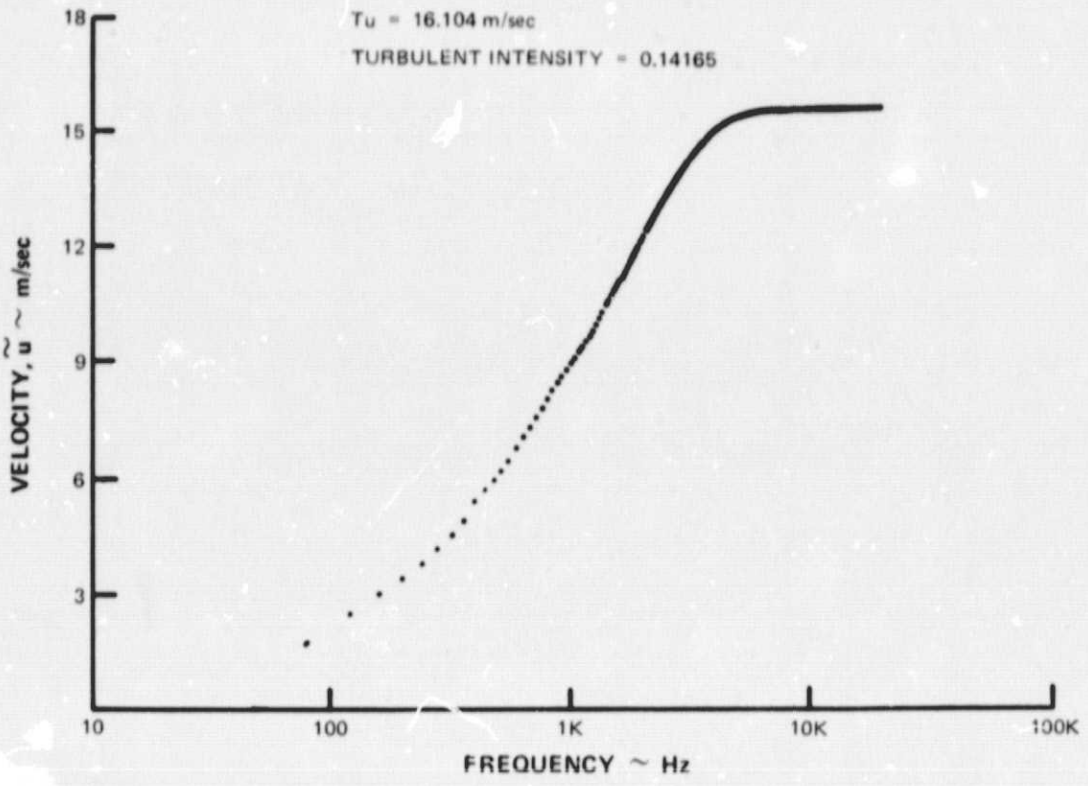


*Figure 23* *Test 3, Probe 4 (Wedge Type) Spectral Distribution for Approach Power Condition at 75 Percent Span*

Macroscale and microscale computed as described in Chapter II are listed in Table VI. The values lie between 0.5 cm and 3.3 cm.

A 3 kHz component corresponds to an axial scale of 3.53 cm. Since 90 percent of the energy in the wave is contained in the 0.1 to 5 kHz bandwidth, the axial length of the fourier components of the velocity wave vary from 0.021 to 1.05 m. The turbulence measured in the diffuser is of quite a large scale. Although the turbulence levels at the 75 percent span were unusually large, there were no qualitative changes between the PSD functions measured at the 25 percent and 50 percent span locations and the 75 percent span.

A distinct peak in the PSD function is observed at blade-passing frequency (about 10kHz) and at higher multiples of blade-passing frequency in some cases. This would be expected in the turbulent flow at any compressor exit for a distance of at least 20 chord lengths behind the rotor.

At idle, evidence of a weak 800 to 900 Hz peak was observed consistently at the 75 percent span location (Figures 22, 24, 25 and 26) and periodically at the 25 percent span location (Figure 21). This peak is unexplained since it lies well above $N_2$ (80 Hz) or $N_1$ (50 Hz) and well below blade-passing frequency (7200 Hz) at this condition.

TABLE VI

TURBULENCE CHARACTERISTICS OF COMPRESSOR DISCHARGE FLOWS

| Hot Film Probe | | | | | | |
|---|---|---|---|---|---|---|
| Number | Percent Span | Angular Location | Tu (meters/sec) | Turbulent Intensity Tu/ū | Λ (Macro-scale In Meters) | λ (Micro-scale In Meters) |
| 2 | 50 | 358° 22′ | 6.782 | 0.06998 | 0.0079 | 0.0051 |
| | | | 8.556 | 0.08160 | 0.0116 | 0.0097 |
| | | | 8.620 | 0.07644 | 0.0083 | 0.0104 |
| | | | 6.471 | 0.06593 | 0.0094 | 0.0078 |
| | | | 9.145 | 0.07958 | 0.0124 | 0.0093 |
| | | | 5.103 | 0.05216 | 0.0169 | 0.0079 |
| 3 | 25 | 17° 52′ | 4.645 | 0.04762 | 0.0153 | 0.0094 |
| | | | 7.560 | 0.06650 | 0.0109 | 0.0076 |
| | | | 4.723 | 0.04782 | 0.0111 | 0.0082 |
| | | | 6.273 | 0.05416 | 0.0107 | 0.0090 |
| | | | 4.710 | 0.04814 | 0.0121 | 0.0089 |
| 1 | 25 | 323° 05′ | 6.725 | 0.06831 | 0.0212 | 0.0087 |
| | | | 8.209 | 0.07695 | 0.0099 | 0.0089 |
| | | | 8.163 | 0.07085 | 0.0086 | 0.0076 |
| | | | 6.774 | 0.06880 | 0.0181 | 0.0077 |
| 2 | 75 | 358° 22′ | 6.890 | 0.07086 | 0.0082 | 0.0079 |
| | | | 11.166 | 0.10557 | 0.0063 | 0.0085 |
| | | | 18.482 | 0.16169 | 0.0100 | 0.0058 |
| | | | 6.834 | 0.07050 | 0.0161 | 0.0071 |
| 4 | 75 | 143° 04′ | 7.683 | 0.07927 | 0.0323 | 0.0064 |
| | | | 11.561 | 0.11026 | 0.0162 | 0.0064 |
| | | | 16.104 | 0.14165 | 0.0104 | 0.0090 |
| | | | 7.807 | 0.08080 | 0.0333 | 0.0086 |
| 6 | 25 | 217° 25′ | 5.747 | 0.05873 | 0.0104 | 0.0081 |
| | | | 6.453 | 0.06136 | 0.0095 | 0.0083 |
| | | | 6.489 | 0.05677 | 0.0088 | 0.0077 |
| | | | 6.007 | 0.06178 | 0.0290 | 0.0072 |

While the origin of the large values of the turbulence cannot be described by the present experimental data, it can be pointed out that the turbulence level at the 75 percent span is large enough to affect airflow from the diffuser to the front end of the burner. For example, if the local ratio of the static pressure across the burner liner, $\Delta P$, and the dynamic pressure of the diffuser flow, q, is 2.5, a ±30 percent (± 2 tu) change in the local velocity will cause the $\Delta P/q$ value to vary from 1.48 to 5.1. The discharge coefficient of the burner liner holes will vary markedly over this range of $\Delta P/q$ values. The scale of turbulence is sufficiently large that significant areas of the burner will be affected simultaneously by the flow perturbations.

Finally, it can be pointed out that the increased turbulence at the O.D. diffuser wall may be useful in improving the performance of the diffuser. Independent measurements show that increasing the turbulence near a diffuser wall can reduce separation of the flow through the additional local mixing caused by the turbulence. A more aggressive diffusion of the gases near the O.D. wall may be possible due to the high level of turbulence in this area.

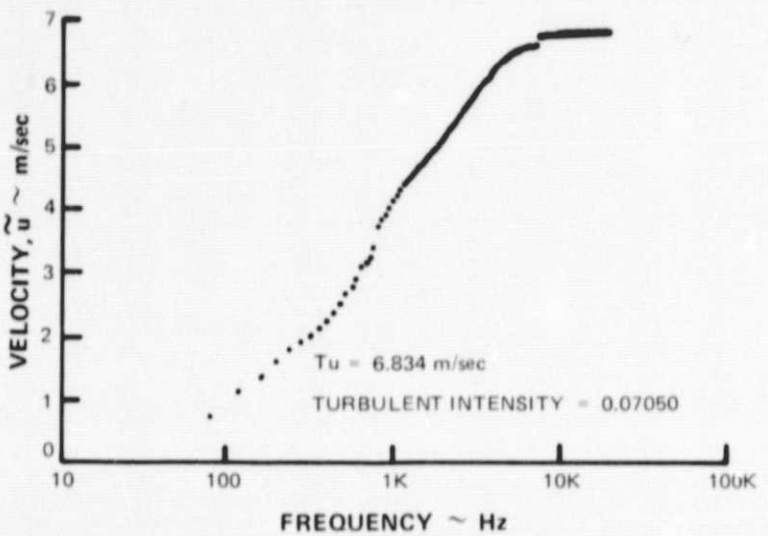


*Figure 24* *Test 3, Probe 2 (Wedge Type) Spectral Distribution for Idle Condition at 75 Percent Span*

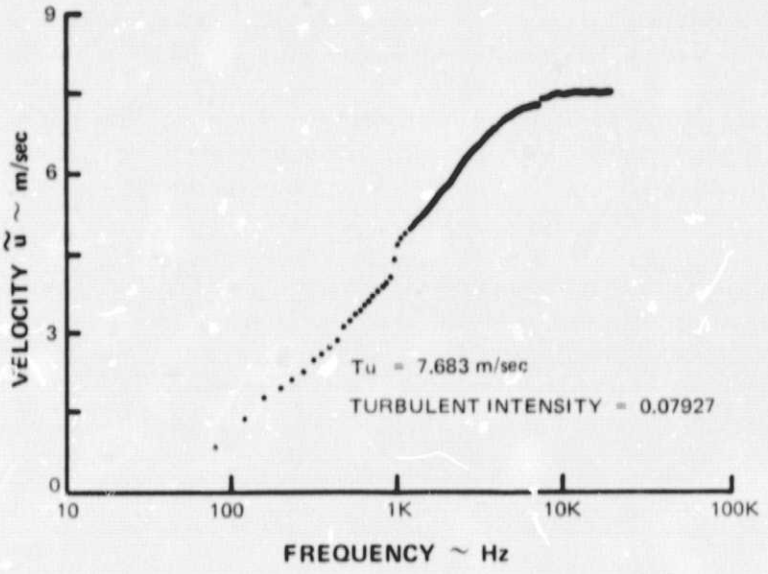


*Figure 25* *Test 3, Probe 4 (Wedge Type) Spectral Distribution for Idle Conaition at 75 Percent Span*

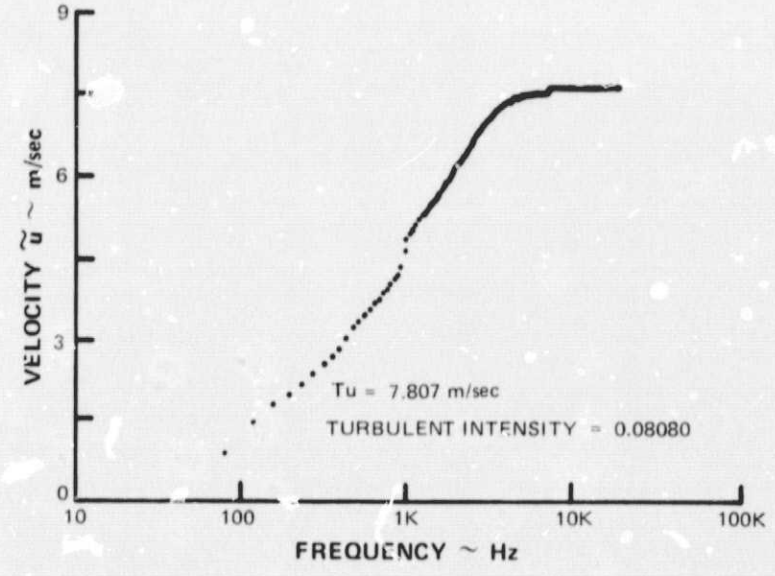


*Figure 26* *Test 3, Probe 4 (Wedge Type) Spectral Distribution for Idle Condition at 75 Percent Span*

## CHAPTER IV

## CONCLUSIONS

The turbulence in the diffuser duct of a large gas turbine has been measured from idle to approach engine conditions. Several features of the turbulence have been documented:

1. The turbulent intensity at the I.D. (25 percent span) and midspan locations increases gradually from 6 ±1 percent at idle to 7 ±1 percent at approach; the turbulent intensity at the O.D. (75 percent span) location increases from 7.5 ±0.5 percent at idle to 15 ±0.5 percent at approach.

2. The energy in the velocity waves is uniformly distributed over a 0.1 to 5 kHz bandwidth. The axial length of the fourier component within this bandwidth varies from 0.021 to 1.05 m.

3. The cut-off frequency of the turbulence (−3 db) is approximately 3 kHz and is not a function of the engine operation. Above the cut-off frequency, the fourier components of the wave decrease at a rate proportional to $f^{-2.5 \pm 0.1}$. Ninety percent of the energy of the waves is contained within a 0.1 to 5 kHz bandwidth.

4. Determination of the origin of the high level of turbulence at the diffuser O.D. requires further information on the development of the turbulence along the diffuser.

5. The turbulence at the diffuser O.D. is of sufficient amplitude and scale to affect the flow to the front end sections of the burner.

6. Velocity fluctuations at blade passing frequency were identified at all span-wise positions. These fluctuations are probably of not sufficient amplitude and scale to affect the flow inside the combustor.

7. Measurements at higher engine power levels are lacking due to sensor probe durability limitations. Data is still needed at higher power levels to determine whether shifts in either the amplitude or scale occur. Use of L.D.V. (Laser Doppler Velocimeter) optical instrumentation should be considered for studies at high power.

## REFERENCES


1. Roberts, R., Fiorentino, A., and Greene, W., "Experimental Clean Combustor Program," Phase III Final Report, NASA CR-135253, October 1977.

2. Heinze, J. O., Turbulence, McGraw Hill, 1959, p. 59.

3. "Heated Sensors in Fluid Flow Measurements", Datametrics, Inc., Wilmington, Mass., Bulletin 600, 1973.